Spontaneous Scattering of Raman Photons from Cavity-QED Systems in the Ultrastrong Coupling Regime

Vincenzo Macrì, Alberto Mercurio, Franco Nori, Salvatore Savasta, and Carlos Sánchez Muñoz

Spontaneous Scattering of Raman Photons from Cavity-QED Systems in the Ultrastrong Coupling Regime

Vincenzo Macr,[1] Alberto Mercurio,[1] Franco Nori,[2,3] Salvatore Savasta,[1, *] and Carlos Sánchez Muñoz[4, †]

[1]*Dipartimento di Scienze Matematiche e Informatiche,*
Scienze Fisiche e Scienze della Terra, Universit di Messina, I-98166 Messina, Italy
[2]*Theoretical Quantum Physics Laboratory, RIKEN Cluster for Pioneering Research, Wakoshi, Saitama 351-0198, Japan*
[3]*RIKEN Center for Quantum Computing (RQC), Wakoshi, Saitama 351-0198, Japan*
[4]*Departamento de Fsica Terica de la Materia Condensada and Condensed Matter Physics Center (IFIMAC),*
Universidad Autnoma de Madrid, 28049 Madrid, Spain
(Dated: November 23, 2022)

We show that spontaneous Raman scattering of incident radiation can be observed in cavity-QED systems without external enhancement or coupling to any vibrational degree of freedom. Raman scattering processes can be evidenced as resonances in the emission spectrum, which become clearly visible as the cavity-QED system approaches the ultrastrong coupling regime. We provide a quantum mechanical description of the effect, and show that ultrastrong light-matter coupling is a necessary condition for the observation of Raman scattering. This effect, and its strong sensitivity to the system parameters, opens new avenues for the characterization of cavity QED setups and the generation of quantum states of light.

The Raman effect describes the inelastic scattering of radiation by matter, in which scattered photons are produced with a frequency which is either lower (Stokes photons) or larger (anti-Stokes photons) than the frequency of the incident field [1–4]. In the context of quantum optics and cavity quantum electrodynamics (cQED), this scattering is usually controlled and stimulated via a second resonant drive [5–14] or a cavity [15–19], constituting the basis of many key techniques of coherent control such as coherent population trapping [5, 6], electromagnetic induced transparency [8, 9] or stimulated Raman adiabatic passage [11–14]. However, the standard observation of *spontaneous* scattering of Raman photons in the absence of any external stimulation typically arises when the illuminating radiation couples to phonons in a material [1–4]. Since this provides a fingerprint of the molecular vibrational modes of the sample, this effect serves as a valuable spectroscopic tool for material characterization [20–25]. Thanks to the plasmonic enhancement of the Raman processes in surface-enhanced Raman spectroscopy [26–28], state-of-the-art experiments have reached regimes where the quantum nature of the vibrational and electromagnetic modes need to be taken into account [29–31], which has led to the field of molecular optomechanics, where a full quantum description of Raman scattering is provided via optomechanical Hamiltonians [32–38].

Here, we demonstrate the intriguing possibility of observing spontaneous Raman scattering in cQED systems in which, in stark contrast to molecular optomechanics, there are no vibrational degrees of freedom. An important feature of the quantum description of Raman scattering is that the underlying process does not conserve the total number of particles: for instance, in a Stokes process, a single laser photon of given energy will become a single, less energetic photon plus a vibrational excitation—a phonon. The underlying Hamiltonian must therefore not conserve the total number of excitations, which is the case in optomechanical interaction Hamiltonians of the form $\hat{V}_{\mathrm{OM}} = g_{\mathrm{OM}}\hat{a}^\dagger\hat{a}(\hat{b}+\hat{b}^\dagger)$ (with $\hat{a}$ and $\hat{b}$ annihilation operators of photon and phonon modes, respectively).

In contrast, let us consider the Hamiltonian describing light-matter interaction between a cavity mode and single dipole, modeled as a two-level system (TLS) with annihilation operator $\hat{\sigma}$. Their coupling is well described by the interaction term of the quantum Rabi model (QRM), $\hat{V} = g(\hat{a}+\hat{a}^\dagger)(\hat{\sigma}+\hat{\sigma}^\dagger)$. The counter-rotating terms in $\hat{V}$ will play no role when the coupling rate is much smaller than the natural frequency of the modes $g \ll \omega_c, \omega_q$, in which case the interaction is well described by the Jaynes-Cummings term $\hat{V} \approx g(\hat{a}\hat{\sigma}^\dagger + \hat{a}^\dagger\hat{\sigma})$ [39, 40]. This interaction term conserves the total number of excitations, and consequently—as we will show—most Raman scattering processes will be forbidden in this regime. The situation changes in the ultrastrong coupling (USC) regime, i.e., the limit where g becomes comparable to ω_c and ω_q and the counter-rotating terms $g(\hat{a}\hat{\sigma}+\hat{a}^\dagger\hat{\sigma}^\dagger)$ play an important role in the dynamics [41, 42]. Similarly to the optomechanical case, the full QRM that describes the dynamics in the USC does not conserve the total number of excitations, and, as a result, this regime features a wealth of exotic nonlinear processes and applications [41–49]. We demonstrate that the observation of spontaneous Raman scattering of photons from an incident field is another characteristic process of the USC regime. In particular, we show unambiguous signatures of these processes in the emission spectra of coherently-driven cQED system in the USC regime [50, 51]. This result establish USC-cQED as a novel scenario where Raman Stokes and anti-Stokes photons are produced spontaneously without any vibrational degree of freedom involved. Beyond exact numerical calculations demonstrating the effect, we support these results with predictions from a full quantum description of the process of Raman scattering.

Model— We consider the cavity QED system sketched in Fig. 1(a), consisting of a single cavity mode of frequency ω_c, driven by a continuous classical field of frequency ω_{L}, and coupled to a point dipole described in the TLS approximation, with a transition frequency ω_q. Since we will be mostly

interested in describing the emission spectrum of such a system, we will resort to the sensor method developed in [52], adding an ancillary sensor qubit of frequency ω_s weakly coupled to the cavity, which has been shown to also produce equivalent results to the quantum-regression theorem in the USC limit [50, 51, 53]. The spectrum of emission at frequency ω_s will thus be proportional to the rate of emission from the sensor qubit.

The Hamiltonian of this system has the form $\hat{H} = \hat{H}_{\text{free}} + \hat{H}_I + \hat{H}_{\text{drive}}$. Setting henceforth $\hbar = 1$, the first term is simply the free Hamiltonian $\hat{H}_{\text{free}} \equiv \omega_c \hat{a}^\dagger \hat{a} + \omega_q \hat{\sigma}_z/2 + \omega_s \hat{\sigma}_z^s/2$, where $\hat{a}$ is the bosonic annihilation operator of the photon field, and $\hat{\sigma}_i$ ($\hat{\sigma}_i^s$) are standard Pauli operators defined on the TLS (sensor) Hilbert space. The second term, $\hat{H}_I$, describes light-matter interaction. In order to write it, we define the polarization operator associated to the TLS and the sensor as $\hat{\mathbf{P}} = (\boldsymbol{\mu}\hat{\sigma}_p + \boldsymbol{\mu}_s \hat{\sigma}_x^s)\delta(\mathbf{r} - \mathbf{r}_0)$, where the TLS operator $\hat{\sigma}_p$ is given by $\hat{\sigma}_p \equiv \cos\theta\hat{\sigma}_x + \sin\theta\hat{\sigma}_z$, and $\boldsymbol{\mu}$ and $\boldsymbol{\mu}_s$ are the respective dipole moments of the TLS and sensor. This definition includes the possibility of a TLS with a permanent dipole moment, parametrized through the angle θ, which breaks the conservation of parity $\hat{\Pi} = \exp[i\pi(\hat{a}^\dagger\hat{a}+\hat{\sigma}_z)]$ and could be induced, e.g., by the flux offset in a flux qubit [43]. In the dipole gauge, the interaction Hamiltonian thus takes the form [54]:

$$\hat{H}_I = i\eta\omega_c(\hat{a}^\dagger - \hat{a})\hat{\sigma}_p + \omega_c\eta_s[i(\hat{a}^\dagger - \hat{a}) + 2\eta\hat{\sigma}_p]\hat{\sigma}_x^s, \quad (1)$$

where η and η_s are the dimensionless coupling parameters between cavity and TLS and sensor, respectively. This Hamiltonian is obtained following the approach in [50, 55, 56], which implements consistently the gauge principle and provides gauge-invariant results even in the presence of approximation such as the truncation of the Hilbert space of the matter system. Finally, the drive Hamiltonian reads $\hat{H}_{\text{drive}}(t) = \Omega[i(\hat{a} - \hat{a}^\dagger) - 2\eta\hat{\sigma}_x]\cos(\omega_{\text{L}}t)$ [50, 51]. Further details on the derivation of this Hamiltonian are provided in the Supplemental Material [57].

Since the setup under consideration is an open quantum system, dissipation must be accounted for by describing the dynamics in terms of a quantum master equation. In the USC regime, the treatment of dissipation, input-output relationships, correlations, driving, and photo-detection rates requires a proper description of the system-bath interaction in terms of the light-matter eigenstates [58–61]. Following the approach in Refs. [51, 62], we write a generalized master equation, which is valid at any light-matter coupling strength (details are given in [57]). In the limit of zero temperature, the master equation reduces to the simple form $\dot{\hat{\rho}} = -i[\hat{H}, \hat{\rho}] + \kappa L_{\hat{\mathcal{X}}^+}[\hat{\rho}] + \gamma L_{\hat{\Sigma}^+}[\hat{\rho}] + \Gamma L_{\hat{\Sigma}_s^+}[\hat{\rho}]$, where $L_{\hat{O}}[\hat{\rho}] \equiv \hat{O}\hat{\rho}\hat{O}^\dagger - \{\hat{O}^\dagger\hat{O}, \hat{\rho}\}/2$ denotes the standard Lindblad terms. Defining $|i\rangle$ as the i-th eigenstate of the full QRM, including the sensor, the decay operators are given by $\hat{\mathcal{X}}^+ = \sum_{j=1}\sum_{k>j}\langle j|[i(\hat{a} - \hat{a}^\dagger) - 2\eta\hat{\sigma}_x]|k\rangle|j\rangle\langle k|$ for the cavity, $\hat{\Sigma}^+ = \hat{\Sigma}^+(\hat{\sigma}, \omega_q)$ for the TLS, and $\hat{\Sigma}_s^+ = \hat{\Sigma}^+(\hat{\sigma}^s, \omega_s)$ for the sensor, where $\hat{\Sigma}^+(\hat{x}, \omega_x) \equiv i\sum_{j=1}\sum_{k>j}\langle j|\hat{x}|k\rangle|j\rangle\langle k|\omega_{kj}/\omega_x$ [57], and κ, γ and Γ are the decay rates of the cavity, TLS and sensor,
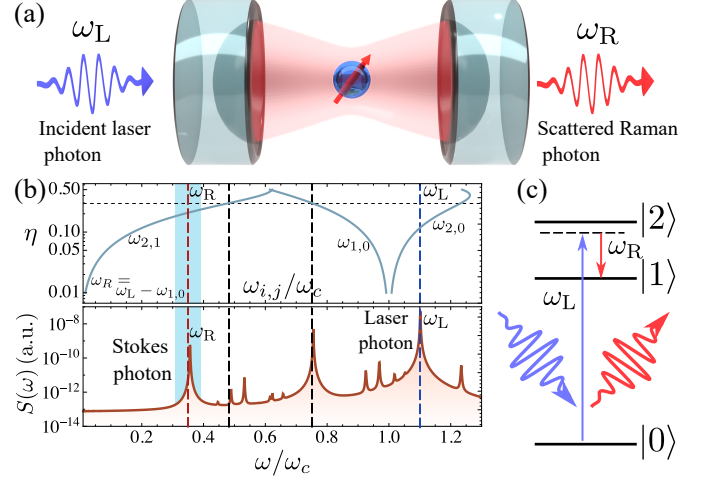

FIG. 1. a) Scheme of the cavity QED system considered in this work: a quantum emitter interacting with a single cavity mode in the ultrastrong-coupling regime and spontaneously scatters a Raman photon from an incident exciting field. (b) Top: Transition energies between the first two excited eigenstates of the light-matter system and the ground state, versus the normalized coupling parameter η. Bottom: Spectrum of emission for $\eta = 0.3$. $\omega_{\text{L}} = 1.1\omega_c$. The red line indicates the frequency at which Stokes photons are emitted, originating from the process sketched in (c).

respectively.

Since counter-rotating terms in $\hat{H}_{\text{drive}}$ cannot be straightforwardly eliminated in the USC regime, the long-time dynamics will yield a time-dependent density matrix oscillating around an average steady state $\hat{\rho}_{\text{ss}} + \delta\hat{\rho}(t)$. Here, we consider the limit of a very small drive $\Omega \ll \eta\omega_c$, so that these oscillations become negligible, and thus we focus on the average steady state $\hat{\rho}_{\text{ss}}$ [57]. We consider that the stationary rate of emission from the sensor is proportional to the spectrum of emission at the sensor's frequency, i.e. $S(\omega_s) \propto \text{Tr}[\hat{\rho}_{\text{ss}}\hat{\Sigma}_s^-\hat{\Sigma}_s^+]$, with the sensor's decay rate Γ corresponding to the filter linewidth.

Scattering of Raman photons— Figure 1(b) depicts an example of the emission spectrum. Here and in the following we fix, unless stated otherwise, $\omega_q = \omega_c$, $\theta = \pi/6$, $\eta = 0.3$, $\eta_s = 10^{-5}$, $\Omega = 5 \times 10^{-3}\omega_c$, $\kappa = \gamma = \Gamma = 10^{-3}\omega_c$, and $\omega_{\text{L}} = 1.1\omega_c$. At first glance, one can observe the presence of a resonance peak at the cavity frequency, and further peaks that match transition energies between the light-matter eigenstates, displayed in the top panel of Fig. 1(b). In addition to these, one can observe an additional peak that corresponds to the spontaneous scattering of a Stokes photon. The corresponding Raman process that gives rise to this peak is sketched in Fig. 1(c). Via a second-order process, an input laser photon of frequency ω_{L} is converted into a lower-energy Raman photon of energy ω_{R} and a light-matter excitation of energy ω_1. Since energy must be conserved in the whole process, the energy of the Stokes photon is expected to be $\omega_{\text{R}} = \omega_{\text{L}} - \omega_1$, and thus it depends linearly with the laser excitation.
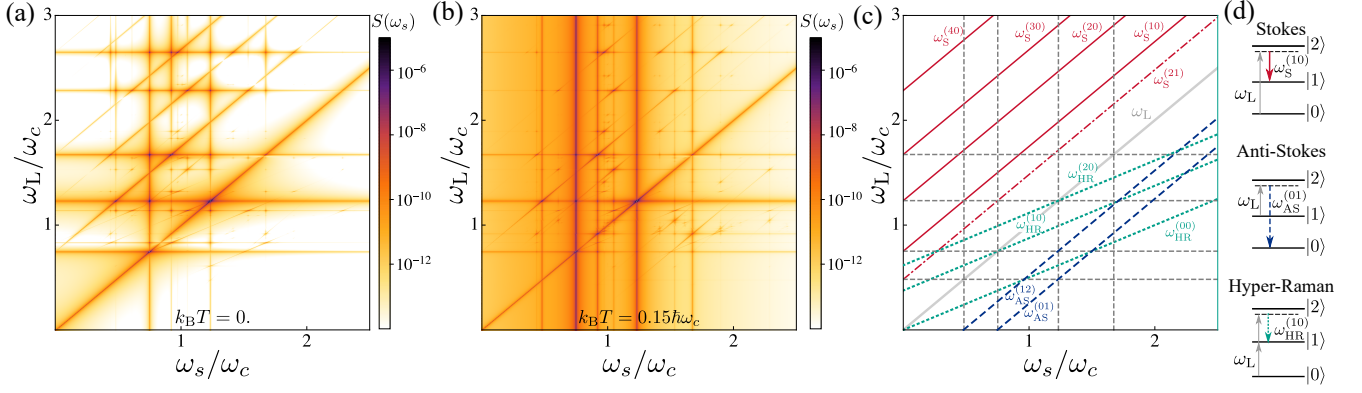
FIG. 2. Emission of Raman photons evidenced through excitation-emission spectra. (a) Excitation-emission spectrum at zero temperature. Raman photons are revealed as diagonal lines (i.e., peaks with frequencies that depend on the laser frequency). (b) Excitation-emission spectrum at non-zero temperature $k_BT = 0.15\hbar\omega_c$. Anti-stokes peaks, which rely on the non-zero population of exited states, are enhanced in this case. (c) Identification of some of the processes seen in panels (a) and (b), which include Stokes (solid,red), anti-Stokes (dashed, blue) and hyper-Raman (dotted, green) photons. Parameters: $\omega_q = \omega_c$, $\theta = \pi/6$, $\eta = 0.3$, $\eta_s = 10^{-5}$, $\Omega = 5 \times 10^{-3}\omega_c$, $\kappa = \gamma = \Gamma = 10^{-3}\omega_c$.

In order to understand the emergence of Raman peaks and its dependence on system parameters such as g or θ, we develop here a full quantum description of the Raman scattering process. To do this, we consider that the cavity is coupled to a broad quasi-continuum of modes with $\hat{H}_b = \sum_q \omega_q \hat{b}_q^\dagger \hat{b}_q$, which will contain the incident radiation field and the scattered Raman photons. The total system Hamiltonian is $\hat{H}_{\text{total}} = \hat{H}_R + \hat{H}_b + \hat{V}_b$, where $\hat{H}_R$ is the quantum Rabi Hamiltonian ($\hat{H}$ above, without the sensor and the drive terms) and $\hat{V}_b = \sum_q g_q(\hat{b}_q + \hat{b}_q^\dagger)\hat{X}$, with $\hat{X} \equiv \hat{a} + \hat{a}^\dagger$. Notice that, in the USC regime, one cannot straightforwardly drop in $\hat{V}_b$ the counter-rotating terms of the form $\hat{b}_q\hat{a}$. A rotating wave approximation can only be done with respect to the positive and negative-frequency parts of $\hat{X}$ in the eigenbasis of the QRM; however, for our current analysis, this approximation is not necessary, and we do not carry it out. In the following, we consider $\hat{H}_R + \hat{H}_b$ as the unperturbed, bare Hamiltonian, and we express $\hat{H}_R$ in diagonal form as $\hat{H}_R = \sum_j \omega_j |j\rangle\langle j|$, where we chose the labeling of the states such that $\omega_k > \omega_j$ for $k > j$. The Raman scattering process can be described by second-order perturbation theory under the constant perturbation $\hat{V}_b$. Let us consider an initial state $|I_i\rangle = |i, n_L, n_R\rangle$, where the first entry labels the eigenstates of $\hat{H}_R$, n_L labels the photon number in the input mode—the laser drive—with frequency ω_L, and n_R indicates the photon number in the output mode of frequency ω_R, where Raman photons are being emitted. We are considering here only the two modes involved in the scattering process; all the other modes of the quasi-continuum are assumed to be in the zero-photon states throughout the process. The energy of the initial state is $\omega_{I,i} = \omega_i + \omega_L n_L + \omega_R n_R$. Then, we consider a final state $|F_f\rangle = |f, n_L - 1, n_R + 1\rangle$, with energy $\omega_{F,f} = \omega_f + \omega_L(n_L - 1) + \omega_R(n_R + 1)$. Energy conservation implies $\omega_{F,f} = \omega_{I,i}$, and, therefore, for a particular choice of initial and final states i and f, the energy of the corresponding

Raman photons is

$$\omega_R = \omega_R^{(f,i)} \equiv \omega_L - (\omega_f - \omega_i). \qquad (2)$$

We stress that this dependence of ω_R with the eigenvalues of the QRM allows to unambiguously identify the origin of these Raman peaks as a pure cQED effect, in contrast to the case of Raman scattering due to coupling to phonons, in which the position of the peaks would be defined by the phonon energy, and therefore would depend on parameters external to the QRM [32]. as we discuss further in [57]. In this process, $|F_f\rangle$ is connected to the initial state $|I_i\rangle$ by a second-order process involving an intermediate virtual state. It is possible to identify two kinds of intermediate states, $|T_1\rangle$ and $|T_2\rangle$, describing respectively the process (i) where a photon is first absorbed from the input state: $|T_1\rangle = |j, n_L - 1, n_R\rangle$, with energy $\omega_{T_1} = \omega_j + \omega_L(n_L - 1) + \omega_R n_R$; and the process (ii) where a photon is first emitted into the output mode: $|T_2\rangle = |j, n_L, n_R + 1\rangle$, with energy $\omega_{T_2} = \omega_j + \omega_L n_L + \omega_R(n_R + 1)$.

The rate of the process $|I_i\rangle \rightarrow |F_f\rangle$ given by the Fermi golden rule, for a given ω_L, i and f, is

$$W_{f,i}(\omega_L, \omega_R) = \frac{2\pi}{\hbar} g_R^2 g_L^2 n_L(n_R + 1)|M_{f,i}|^2 \delta(\omega_R - \omega_R^{(f,i)}), \qquad (3)$$

where $\omega_{f,i} = \omega_f - \omega_i$ and

$$M_{f,i}(\omega_L, \omega_R) = \sum_j \left(\frac{X_{f,j}X_{j,i}}{\omega_{T_1} - \omega_{I_i}} + \frac{X_{f,j}X_{j,i}}{\omega_{T_2} - \omega_{I_i}} \right), \qquad (4)$$

with $X_{f,j} \equiv \langle f|(\hat{a} + \hat{a}^\dagger)|j\rangle$. Notice that $\omega_{T_1} - \omega_{I,i} = \omega_{j,i} - \omega_L$, and $\omega_{T_2} - \omega_{I,i} = \omega_{j,i} + \omega_R^{(f,i)}$. The total scattering rate for the process is obtained by summing over all possible initial and final states, which will be constrained by the energy-conservation condition in Eq. (3), giving

$$W(\omega_L, \omega_R) = \sum_{f,i} W_{f,i}(\omega_L, \omega_R)\rho_i^{ss}(1 - \rho_f^{ss}), \qquad (5)$$

where ρ_k^{ss} is the steady-state occupation probability of the eigenstate $|k\rangle$ of $\hat{H}_R$. For a system at very low temperatures and low driving which is mostly in the ground state, so that $\rho_0^{\mathrm{ss}} \approx 1$, we obtain $W(\omega_{\mathrm{L}}, \omega_{\mathrm{R}}) = \sum_f W_{f,0}(\omega_{\mathrm{L}}, \omega_{\mathrm{R}})$. Therefore, if Raman spectroscopy is performed by probing cQED systems that are close to the ground state, only the family of Raman processes that start from $|0\rangle$ are expected to be observed.

Visibility of Raman processes—. The quantum scattering process outlined above manifests as resonances in the spectrum of emission, centered at the frequencies $\omega_{\mathrm{R}}^{(f,i)}$, and are clearly identified when this spectrum is represented versus the excitation frequency in the form of an excitation-emission spectrum. Numerical calculations of excitation-emission spectra at two different temperatures are shown in Fig. 2(a-b). Raman peaks have a characteristic feature that distinguishes them from peaks arising from standard radiative transitions: their central frequency $\omega_{\mathrm{R}}^{(f,i)}$ depends linearly on the laser frequency ω_{L}, manifesting as diagonal lines in the excitation-emission spectrum. The Raman peaks that are most clearly identified in Fig. 2(a-b) are labeled in Fig. 2(c). At low temperatures, the most visible ones are Stokes processes that start at the ground state of the light-matter system and end at some excited state $|f\rangle$ (we label these Stokes processes as $\omega_{\mathrm{S}}^{(f0)}$). In agreement to what is expected from Eq. (5), at small temperatures, Stokes processes that start in an excited state are hardly visible or not visible at all; in Fig. 2(c) we highlight the process $\omega_{\mathrm{S}}^{(21)}$—starting in $|1\rangle$ and finishing in $|2\rangle$—which is the one that can be recognized in certain regions of the spectra shown. Likewise, the emission of anti-Stokes photons with frequencies larger than the drive frequency is only clearly visible at finite temperatures: these processes require the energy of the final state of the cQED system to be lower than the initial one, and therefore, the initial state needs to be an excited state with a non-negligible stationary occupation probability. These calculations also show that higher-order, hyper-Raman processes are faintly visible as well in the excitation emission spectra. These processes scatter two incident laser photons into a Raman photon, and therefore conservation of energy establishes that the frequency of the hyper-Raman photons must be $\omega_{\mathrm{R}}^{(fi)} = 2\omega_{\mathrm{L}} - (\omega_f - \omega_i)$. Such processes are then identified in the excitation-emission spectra as straight lines with twice the slope of standard Raman processes.

All the features just outlined are clearer when one approaches the ultra-strong coupling regime of light-matter interaction, $\eta \sim 0.1$, so that the matrix elements $X_{k,j}$ in Eq. (3) acquire sizable values. Indeed, Fig. 3(a) shows the calculation of the scattering rate W versus η computed through Eq. (5) for the Stokes process $|0\rangle \to |1\rangle$, which is the most visible one in a system close to the ground state, compared to the intensity of the corresponding Raman peak computed in the excitation emission spectra. Beyond the good agreement between both results, which supports our description of the underlying quantum process, we highlight the exponential increase of the intensity of the peak with η. Way bellow the USC regime, the small values of the scattering rate would make observing Raman processes in cavity QED systems very challenging, as shown in Fig. 3(c), where for $\eta = 0.01$ the first Stokes peak is extremely hard to notice.

It is illustrative to consider the possibility of Raman processes in a cQED system with $\eta \ll 1$, therefore well described by a Jaynes-Cummings Hamiltonian. The eigenstates of this system are organized in doublets $|j_\pm\rangle$ that are also eigenstates of the total number of excitations $\hat{N} = \hat{a}^\dagger \hat{a} + \hat{\sigma}^\dagger \hat{\sigma}$, i.e. $\hat{N}|j_\pm\rangle = j|j_\pm\rangle$. This means that the only Raman processes allowed are those that conserve the total number of excitations, i.e., those whose initial and final states are within the same doublet. Since processes that start and end in the ground state yield $\omega_{\mathrm{R}} = \omega_{\mathrm{L}}$ and therefore do not produce energy-shifted photons, the observation of the most relevant Raman processes that involve the ground state is not possible in Jaynes Cummings system. Peaks that may be observed in this limit, such as ω_{S}^{21} and $\omega_{\mathrm{AS}}^{21}$, are only vaguely visible even in the ultrastrong-coupling regime, as can be seen in Fig. 2(a,b), and would require a stationary population of excited states, whose origin can imply extra sources of dephasing. We therefore conclude that emission of Raman photons from coherently driven cavity QED systems is essentially a characteristic effect of the USC coupling limit.

The presence or absence of certain Raman peaks also provides information about microscopic parameters, such as the static dipole moment parametrized by θ. Each peak exhibits a characteristic dependence on θ, as we illustrate in Fig. 3(b)
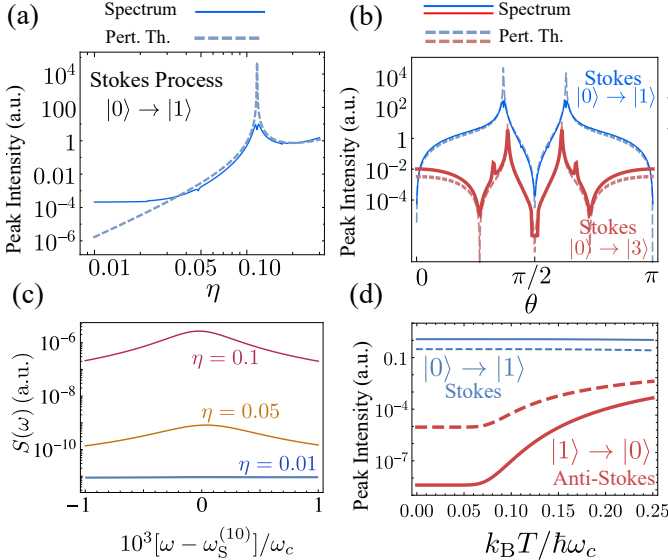

FIG. 3. (a) Intensity of the Raman peak $\omega_{\mathrm{R}}^{(10)}$ and corresponding scattering rate from Fermi's Golden rule. $\theta = \pi/6$. (b) Raman intensity versus θ for two types Stokes processes. (c) Spectrum around Raman resonance $\omega_{\mathrm{S}}^{(10)}$ for increasing η. (d) Raman intensity versus temperature for a Stokes process and an anti-Stokes process.

with two particular examples, the Stokes peaks $\omega_{\mathrm{S}}^{(10)}$ and $\omega_{\mathrm{S}}^{(30)}$, showing that this dependence is well captured by our quantum description of the process based on perturbation theory. This example highlights that, in some cases—such as for $\omega_{\mathrm{R}}^{(10)}$—the breaking of parity symmetry ($\theta \neq 0$) is necessary to observe the corresponding Raman peak. For $\theta = 0$, eigenstates of the QRM are also parity eigenstates, and thus only Raman processes that conserve parity, such as $|0\rangle \rightarrow |3\rangle$, will have a non-zero scattering rate.

Finally, Fig. 3(d) shows that our quantum model provides a good qualitative prediction for the different dependence of Stokes and anti-Stokes peaks on temperature, showing that the intensity Stokes peaks is just slightly reduced, while the intensity of anti-Stokes peaks can be increased by orders of magnitude, explained by the corresponding increase of the stationary population of excited states.

Conclusions—. We have demonstrated that spontaneous scattering of Raman photons from cQED systems can be visible in the USC regime without involving any vibrational degree of freedom. This result introduces news fingerprints of strong light-matter interaction that will allow to leverage the potential of Raman spectroscopy for system characterization in the field of cQED. The findings that we describe should be readily observable in superconducting circuits platforms, where couplings between single qubits and microwave resonators exceeding $\eta > 0.1$ have been reported [63–66]. The study of quantum correlations in Raman photons can also offer new routes for the generation of non-classical light [58, 67–70].

---

* ssavasta@unime.it

† carlos.sanchezmunnoz@uam.es

[1] C. V. Raman and K. S. Krishnan, A New Type of Secondary Radiation, Nature **121**, 501 (1928).

[2] C. V. Raman, A new radiation, Proceedings of the Indian Academy of Sciences - Section A **37**, 333 (1953).

[3] D. A. Long, *The Raman Effect: A Unified Treatment of the Theory of Raman Scattering by Molecules* (John Wiley & Sons, Ltd, Chichester, UK, 2002).

[4] A. Fainstein, B. Jusserand, and V. Thierry-Mieg, Cavity-Polariton Mediated Resonant Raman Scattering, Physical Review Letters **78**, 1576 (1997).

[5] P. Jamonneau, G. Hétet, A. Dréau, J.-F. Roch, and V. Jacques, Coherent Population Trapping of a Single Nuclear Spin Under Ambient Conditions, Physical Review Letters **116**, 043603 (2016).

[6] A. Donarini, M. Niklas, M. Schafberger, N. Paradiso, C. Strunk, and M. Grifoni, Coherent population trapping by dark state formation in a carbon nanotube quantum dot, Nature Communications **10**, 381 (2019).

[7] N. V. Vitanov, A. A. Rangelov, B. W. Shore, and K. Bergmann, Stimulated Raman adiabatic passage in physics, chemistry, and beyond, Reviews of Modern Physics **89**, 015006 (2017).

[8] M. Fleischhauer, A. Imamoglu, and P. J. Marangos, Electromagnetically induced transparency, Reviews of Modern Physics **77**, 633 (2005).

[9] J. Long, H. S. Ku, X. Wu, X. Gu, R. E. Lake, M. Bal, Y. X. Liu, and D. P. Pappas, Electromagnetically Induced Transparency in Circuit Quantum Electrodynamics with Nested Polariton States, Physical Review Letters **120**, 083602 (2018).

[10] Y. Guo, C.-C. Shu, D. Dong, and F. Nori, Vanishing and Revival of Resonance Raman Scattering, Physical Review Letters **123**, 223202 (2019).

[11] L. F. Wei, J. R. Johansson, L. X. Cen, S. Ashhab, and F. Nori, Controllable Coherent Population Transfers in Superconducting Qubits for Quantum Computing, Physical Review Letters **100**, 113601 (2008).

[12] C.-C. Shu, J. Yu, K.-J. Yuan, W.-H. Hu, J. Yang, and S.-L. Cong, Stimulated Raman adiabatic passage in molecular electronic states, Physical Review A **79**, 023418 (2009).

[13] K. S. Kumar, A. Vepsäläinen, S. Danilin, and G. S. Paraoanu, Stimulated Raman adiabatic passage in a three-level superconducting circuit, Nature Communications **7**, 10628 (2016).

[14] G. Falci, P. G. Di Stefano, A. Ridolfo, A. D'Arrigo, G. S. Paraoanu, and E. Paladino, Advances in quantum control of three-level superconducting circuit architectures, Fortschritte der Physik **65**, 1600077 (2017).

[15] F. Dimer, B. Estienne, A. S. Parkins, and H. J. Carmichael, Proposed realization of the Dicke-model quantum phase transition in an optical cavity QED system, Physical Review A **75**, 013804 (2007).

[16] S. Sun, J. L. Zhang, K. A. Fischer, M. J. Burek, C. Dory, K. G. Lagoudakis, Y.-K. Tzeng, M. Radulaski, Y. Kelaita, A. Safavi-Naeini, Z.-X. Shen, N. A. Melosh, S. Chu, M. Lončar, and J. Vučković, Cavity-Enhanced Raman Emission from a Single Color Center in a Solid, Physical Review Letters **121**, 083601 (2018).

[17] M. Hennrich, T. Legero, A. Kuhn, and G. Rempe, Vacuum-Stimulated Raman Scattering Based on Adiabatic Passage in a High-Finesse Optical Cavity, Physical Review Letters **85**, 4872 (2000).

[18] A. Kuhn, M. Hennrich, and G. Rempe, Deterministic Single-Photon Source for Distributed Quantum Networking, Physical Review Letters **89**, 067901 (2002).

[19] T. M. Sweeney, S. G. Carter, A. S. Bracker, M. Kim, C. S.

Kim, L. Yang, P. M. Vora, P. G. Brereton, E. R. Cleveland, and D. Gammon, Cavity-stimulated Raman emission from a single quantum dot spin, Nature Photonics **8**, 442 (2014).

[20] A. Orlando, F. Franceschini, C. Muscas, S. Pidkova, M. Bartoli, M. Rovere, and A. Tagliaferro, A Comprehensive Review on Raman Spectroscopy Applications, Chemosensors **9**, 262 (2021).

[21] A. Kudelski, Analytical applications of Raman spectroscopy, Talanta **76**, 1 (2008).

[22] B. Pettinger, P. Schambach, C. J. Villagómez, and N. Scott, Tip-Enhanced Raman Spectroscopy: Near-Fields Acting on a Few Molecules, Annual Review of Physical Chemistry **63**, 379 (2012).

[23] X.-M. Qian and S. M. Nie, Single-molecule and single-nanoparticle SERS: from fundamental mechanisms to biomedical applications, Chemical Society Reviews **37**, 912 (2008).

[24] D. Yang and Y. Ying, Applications of Raman Spectroscopy in Agricultural Products and Food Analysis: A Review, Applied Spectroscopy Reviews **46**, 539 (2011).

[25] V. Poornima Parvathi, R. Parimaladevi, V. Sathe, and U. Mahalingam, Graphene boosted silver nanoparticles as surface enhanced Raman spectroscopic sensors and photocatalysts for removal of standard and industrial dye contaminants, Sensors and Actuators B: Chemical **281**, 679 (2019).

[26] K. Kneipp, Y. Wang, H. Kneipp, L. T. Perelman, I. Itzkan, R. R. Dasari, and M. S. Feld, Single Molecule Detection Using Surface-Enhanced Raman Scattering (SERS), Physical Review Letters **78**, 1667 (1997).

[27] S. Nie and S. R. Emory, Probing Single Molecules and Single Nanoparticles by Surface-Enhanced Raman Scattering, Science **275**, 1102 (1997).

[28] J. Langer, D. Jimenez de Aberasturi, J. Aizpurua, R. A. Alvarez-Puebla, B. Auguié, J. J. Baumberg, G. C. Bazan, S. E. J. Bell, A. Boisen, A. G. Brolo, J. Choo, D. Cialla-May, V. Deckert, L. Fabris, K. Faulds, F. J. García de Abajo, R. Goodacre, D. Graham, A. J. Haes, C. L. Haynes, C. Huck, T. Itoh, M. Käll, J. Kneipp, N. A. Kotov, H. Kuang, E. C. Le Ru, H. K. Lee, J.-F. Li, X. Y. Ling, S. A. Maier, T. Mayerhöfer, M. Moskovits, K. Murakoshi, J.-M. Nam, S. Nie, Y. Ozaki, I. Pastoriza-Santos, J. Perez-Juste, J. Popp, A. Pucci, S. Reich, B. Ren, G. C. Schatz, T. Shegai, S. Schlücker, L.-L. Tay, K. G. Thomas, Z.-Q. Tian, R. P. Van Duyne, T. Vo-Dinh, Y. Wang, K. A. Willets, C. Xu, H. Xu, Y. Xu, Y. S. Yamamoto, B. Zhao, and L. M. Liz-Marzán, Present and Future of Surface-Enhanced Raman Scattering, ACS Nano **14**, 28 (2020).

[29] R. Zhang, Y. Zhang, Z. C. Dong, S. Jiang, C. Zhang, L. G. Chen, L. Zhang, Y. Liao, J. Aizpurua, Y. Luo, J. L. Yang, and J. G. Hou, Chemical mapping of a single molecule by plasmon-enhanced Raman scattering, Nature **498**, 82 (2013).

[30] W. Zhu and K. B. Crozier, Quantum mechanical limit to plasmonic enhancement as observed by surface-enhanced Raman scattering, Nature Communications **5**, 5228 (2014).

[31] A. Shalabney, J. George, J. Hutchison, G. Pupillo, C. Genet, and T. W. Ebbesen, Coherent coupling of molecular resonators with a microcavity mode, Nature Communications **6**, 5981 (2015).

[32] M. K. Schmidt, R. Esteban, A. González-Tudela, G. Giedke, and J. Aizpurua, Quantum Mechanical Description of Raman Scattering from Molecules in Plasmonic Cavities, ACS Nano **10**, 6291 (2016).

[33] P. Roelli, C. Galland, N. Piro, and T. J. Kippenberg, Molecular cavity optomechanics as a theory of plasmon-enhanced Raman scattering, Nature Nanotechnology **11**, 164 (2016).

[34] M. Kamandar Dezfouli and S. Hughes, Quantum Optics Model of Surface-Enhanced Raman Spectroscopy for Arbi-
trarily Shaped Plasmonic Resonators, ACS Photonics **4**, 1045 (2017).

[35] M. K. Dezfouli, R. Gordon, and S. Hughes, Molecular Optomechanics in the Anharmonic Cavity-QED Regime Using Hybrid MetalDielectric Cavity Modes, ACS Photonics **6**, 1400 (2019).

[36] S. Hughes, A. Settineri, S. Savasta, and F. Nori, Resonant Raman scattering of single molecules under simultaneous strong cavity coupling and ultrastrong optomechanical coupling in plasmonic resonators: Phonon-dressed polaritons, Physical Review B **104**, 045431 (2021).

[37] P. Roelli, D. Martin-Cano, T. J. Kippenberg, and C. Galland, Molecular Platform for Frequency Upconversion at the Single-Photon Level, Physical Review X **10**, 031057 (2020).

[38] B. Gurlek, V. Sandoghdar, and D. Martin-Cano, Engineering Long-Lived Vibrational States for an Organic Molecule, Physical Review Letters **127**, 123603 (2021).

[39] M. O. Scully and M. S. Zubairy, *Quantum optics* (Cambridge University Press, 2002).

[40] G. S. Agarwal, *Quantum optics* (Cambridge University Press, 2012).

[41] A. Frisk Kockum, A. Miranowicz, S. De Liberato, S. Savasta, and F. Nori, Ultrastrong coupling between light and matter, Nature Reviews Physics **1**, 19 (2019).

[42] P. Forn-Díaz, L. Lamata, E. Rico, J. Kono, and E. Solano, Ultrastrong coupling regimes of light-matter interaction, Reviews of Modern Physics **91**, 025005 (2019).

[43] T. Niemczyk, F. Deppe, H. Huebl, E. P. Menzel, F. Hocke, M. J. Schwarz, J. J. Garcia-Ripoll, D. Zueco, T. Hümmer, E. Solano, A. Marx, and R. Gross, Circuit quantum electrodynamics in the ultrastrong-coupling regime, Nature Physics **6**, 772 (2010).

[44] K. K. W. Ma and C. K. Law, Three-photon resonance and adiabatic passage in the large-detuning Rabi model, Physical Review A **92**, 023842 (2015).

[45] L. Garziano, R. Stassi, V. Macrì, A. F. Kockum, S. Savasta, and F. Nori, Multiphoton quantum Rabi oscillations in ultrastrong cavity QED, Physical Review A **92**, 063830 (2015).

[46] L. Garziano, V. Macrì, R. Stassi, O. Di Stefano, F. Nori, and S. Savasta, One Photon Can Simultaneously Excite Two or More Atoms, Physical Review Letters **117**, 043601 (2016).

[47] R. Stassi, V. Macrì, A. F. Kockum, O. Di Stefano, A. Miranowicz, S. Savasta, and F. Nori, Quantum nonlinear optics without photons, Physical Review A **96**, 023818 (2017).

[48] A. F. Kockum, A. Miranowicz, V. Macrì, S. Savasta, and F. Nori, Deterministic quantum nonlinear optics with single atoms and virtual photons, Physical Review A **95**, 063849 (2017).

[49] A. F. Kockum, V. Macrì, L. Garziano, S. Savasta, and F. Nori, Frequency conversion in ultrastrong cavity QED, Scientific Reports **7**, 5313 (2017).

[50] W. Salmon, C. Gustin, A. Settineri, O. Di Stefano, D. Zueco, S. Savasta, F. Nori, and S. Hughes, Gauge-independent emission spectra and quantum correlations in the ultrastrong coupling regime of open system cavity-QED, Nanophotonics **11**, 1573 (2022).

[51] A. Mercurio, V. Macrì, C. Gustin, S. Hughes, S. Savasta, and F. Nori, Regimes of Cavity-QED under Incoherent Excitation: From Weak to Deep Strong Coupling, Physical Review Research **4**, 023048 (2021).

[52] E. del Valle, A. Gonzalez-Tudela, F. P. Laussy, C. Tejedor, and M. J. Hartmann, Theory of Frequency-Filtered and Time-Resolved N-Photon Correlations, Physical Review Letters **109**, 183601 (2012).

[53] W. Salmon, *Master Equations for Computing Gauge-Invariant Observables in the Ultrastrong Coupling Regime of Cavity-*

QED, Doctoral dissertation, Queen's University (Canada) (2021).

[54] A. Settineri, O. Di Stefano, D. Zueco, S. Hughes, S. Savasta, and F. Nori, Gauge freedom, quantum measurements, and time-dependent interactions in cavity QED, Physical Review Research **3**, 023079 (2021).

[55] D. De Bernardis, P. Pilar, T. Jaako, S. De Liberato, and P. Rabl, Breakdown of gauge invariance in ultrastrong-coupling cavity QED, Physical Review A **98**, 053819 (2018).

[56] O. Di Stefano, A. Settineri, V. Macrì, L. Garziano, R. Stassi, S. Savasta, and F. Nori, Resolution of gauge ambiguities in ultrastrong-coupling cavity quantum electrodynamics, Nature Physics **15**, 803 (2019).

[57] See Supplemental Material for further details on the derivation of the Quantum Rabi Model Hamiltonian in the dipole gauge, the derivation of the master equation on the dressed-operator approach, the calculation of time-averaged density matrix form time-dependent Liouvillians using the Floquet method, and the significance of Raman peaks for the spectroscopy of cavity QED systems, which includes references [71–83].

[58] A. Ridolfo, M. Leib, S. Savasta, and M. J. Hartmann, Photon Blockade in the Ultrastrong Coupling Regime, Physical Review Letters **109**, 193602 (2012).

[59] F. Beaudoin, J. M. Gambetta, and A. Blais, Dissipation and ultrastrong coupling in circuit QED, Physical Review A **84**, 043832 (2011).

[60] O. Di Stefano, A. F. Kockum, A. Ridolfo, S. Savasta, and F. Nori, Photodetection probability in quantum systems with arbitrarily strong light-matter interaction, Scientific Reports **8**, 17825 (2018).

[61] A. Le Boité, Theoretical Methods for Ultrastrong Light-Matter Interactions, Advanced Quantum Technologies **3**, 1900140 (2020).

[62] A. Settineri, V. Macrí, A. Ridolfo, O. Di Stefano, A. F. Kockum, F. Nori, and S. Savasta, Dissipation and thermal noise in hybrid quantum systems in the ultrastrong-coupling regime, Physical Review A **98**, 053834 (2018).

[63] P. Forn-Díaz, G. Romero, C. J. P. M. Harmans, E. Solano, and J. E. Mooij, Broken selection rule in the quantum Rabi model, Scientific Reports **6**, 26720 (2016).

[64] F. Yoshihara, T. Fuse, S. Ashhab, K. Kakuyanagi, S. Saito, and K. Semba, Superconducting qubit–oscillator circuit beyond the ultrastrong-coupling regime, Nature Physics **13**, 44 (2017).

[65] F. Yoshihara, T. Fuse, S. Ashhab, K. Kakuyanagi, S. Saito, and K. Semba, Characteristic spectra of circuit quantum electrodynamics systems from the ultrastrong- to the deep-strong-coupling regime, Physical Review A **95**, 053824 (2017).

[66] F. Yoshihara, T. Fuse, Z. Ao, S. Ashhab, K. Kakuyanagi, S. Saito, T. Aoki, K. Koshino, and K. Semba, Inversion of Qubit Energy Levels in Qubit-Oscillator Circuits in the Deep-Strong-Coupling Regime, Physical Review Letters **120**, 183601 (2018).

[67] A. Faraon, I. Fushman, D. Englund, N. Stoltz, P. Petroff, and J. Vučković, Coherent generation of non-classical light on a chip via photon-induced tunnelling and blockade, Nature Physics **4**, 859 (2008).

[68] D. E. Chang, V. Vuletić, and M. D. Lukin, Quantum nonlinear optics photon by photon, Nature Photonics **8**, 685 (2014).

[69] K. Müller, A. Rundquist, K. A. Fischer, T. Sarmiento, K. G. Lagoudakis, Y. A. Kelaita, C. Sánchez Muñoz, E. del Valle, F. P. Laussy, and J. Vučković, Coherent Generation of Nonclassical Light on Chip via Detuned Photon Blockade, Physical Review Letters **114**, 233601 (2015).

[70] C. Hamsen, K. N. Tolazzi, T. Wilk, and G. Rempe, Two-Photon Blockade in an Atom-Driven Cavity QED System, Physical Review Letters **118**, 133604 (2017).

[71] S. Savasta, O. Di Stefano, and F. Nori, Thomas–reiche–kuhn (trk) sum rule for interacting photons, Nanophotonics **10**, 465 (2021).

[72] A. Majumdar, A. Papageorge, E. D. Kim, M. Bajcsy, H. Kim, P. Petroff, and J. Vučković, Probing of single quantum dot dressed states via an off-resonant cavity, Physical Review B **84**, 085310 (2011).

[73] A. Papageorge, A. Majumdar, E. D. Kim, and J. Vučković, Bichromatic driving of a solid-state cavity quantum electrodynamics system, New Journal of Physics **14**, 013028 (2012).

[74] M. Maragkou, C. Sánchez-Muñoz, S. Lazić, E. Chernysheva, H. P. van der Meulen, A. González-Tudela, C. Tejedor, L. J. Martínez, I. Prieto, P. A. Postigo, and J. M. Calleja, Bichromatic dressing of a quantum dot detected by a remote second quantum dot, Physical Review B **88**, 075309 (2013).

[75] M. G. Paris, Quantum estimation for quantum technology, International Journal of Quantum Information **7**, 125 (2009).

[76] H. M. Wiseman and G. J. Milburn, *Quantum Measurement and Control* (Cambridge University Press, Cambridge, 2009).

[77] J. P. Dowling and K. P. Seshadreesan, Quantum optical technologies for metrology, sensing, and imaging, Journal of Lightwave Technology **33**, 2359 (2015).

[78] C. Ghinea, Introduction To Quantum Fisher Information, in *Quantum Probability and Related Topics* (World Scientific, 2011) pp. 261–281.

[79] A. Luis, Fisher information as a generalized measure of coherence in classical and quantum optics, Optics Express **20**, 24686 (2012).

[80] J. Chao, E. Sally Ward, and R. J. Ober, Fisher information theory for parameter estimation in single molecule microscopy: tutorial, Journal of the Optical Society of America A **33**, B36 (2016).

[81] D. Šafránek, Simple expression for the quantum Fisher information matrix, Physical Review A **97**, 042322 (2018).

[82] J. Liu, H. Yuan, X.-M. Lu, and X. Wang, Quantum Fisher information matrix and multiparameter estimation, Journal of Physics A: Mathematical and Theoretical **53**, 023001 (2020).

[83] A. Vivas-Viaña and C. Sánchez Muñoz, Two-photon resonance fluorescence of two interacting nonidentical quantum emitters, Physical Review Research **3**, 033136 (2021).